New Phytologist

Research

The unique root form and function on the Tibetan Plateau

Zhi Zheng[1], Feifei Dong[1], Ziyue Li[2,3], Lijuan Chen[1], Qinwen Han[4], Monique Weemstra[5], J. Aaron Hogan[6,7], Oscar J. Valverde-Barrantes[8], Wen-Hao Zhang[2,3], Junjian Wang[9,10], Junxiang Ding[11] and Deliang Kong[4]

[1]College of Life Science, Northwest Normal University, Lanzhou, 730070, China; [2]State Key Laboratory of Vegetation and Environmental Change, Institute of Botany, Chinese Academy of Sciences, Beijing, 100093, China; [3]College of Resources and Environment, University of Chinese Academy of Sciences, Beijing, 100049, China; [4]College of Forestry, Henan Agricultural University, Zhengzhou, 450046, China; [5]Forest Ecology and Forest Management Group, Wageningen University, 6700 AA, Wageningen, the Netherlands; [6]Department of Biology, Colorado State University, Fort Collins, CO 80523, USA; [7]Department of Ecology and Conservation Biology, Texas A&M University, College Station, TX 77843, USA; [8]International Center of Tropical Botany, Florida International University, Miami, Florida 33199, USA; [9]State Key Laboratory of Soil Pollution Control and Safety, School of Environmental Science and Engineering, Southern University of Science and Technology, Shenzhen, 518055, China; [10]Guangdong Provincial Key Laboratory of Soil and Groundwater Pollution Control, School of Environmental Science and Engineering, Southern University of Science and Technology, Shenzhen, 518055, China; [11]College of Ecology and Environment, Zhengzhou University, Zhengzhou, 450001, China

Authors for correspondence:
Deliang Kong
Email: deliangkong1999@126.com

Zhi Zheng
Email: zhengzhi1982@126.com

Received: *13 June 2025*
Accepted: *10 September 2025*

New Phytologist (2025)
doi: 10.1111/nph.70595

Key words: alpine ecosystem, anatomical traits, herbaceous plants, root exudation rate, specific root respiration.

Summary

- Root traits, particularly anatomical traits, underpin root functions necessary for plant survival and adaptation. However, the coordination of root traits in extreme environments remains unresolved.
- We linked root functions that encompass foraging, uptake, and mining to anatomical traits of absorptive roots of typical and common species on the Tibetan Plateau and compared them with those in other regions globally.
- Our results showed that in alpine grasslands of the Tibetan Plateau, root functions were governed by root diameter and associated anatomical traits, rather than by specific root length (SRL, an indicator of root foraging) as observed globally. Specific root respiration (an indicator of active nutrient uptake) scaled with tube size and number within the root vascular system, whereas root exudation rate and acid phosphatase activity (indicators of nutrient mining) were linked to cortex cell size and layer number. These anatomical adaptations contrast with global patterns, where higher SRL supports nutrient acquisition through reduced construction costs.
- Our findings reveal unique root forms and functions in the alpine environments, highlighting the importance of cellular anatomy in shaping plant function in extreme environments.

Introduction

Plant species have evolved a wide range of forms and functions that allow them to cope with heterogeneous environments (Díaz *et al.*, 2016; Carmona *et al.*, 2021; Laughlin *et al.*, 2021; Weigelt *et al.*, 2023; Yang *et al.*, 2025). Among these functions, nutrient acquisition is a fundamental driver of plant performance and ecosystem functioning. Therefore, uncovering patterns and mechanisms underlying interspecific variation in these absorptive root traits is critical for understanding the formation and maintenance of plant diversity and plant responses and adaptation to environmental changes (Ma *et al.*, 2018; Carmona *et al.*, 2021).

Root nutrient acquisition involves three interrelated processes: each connecting with distinct root traits that vary considerably across species. First, root foraging refers to the proliferation of roots in soil to contact nutrients by the root epidermis (Ding *et al.*, 2023; Zhang *et al.*, 2023; Zhao *et al.*, 2024). Root foraging capacity is strongly related to root diameter and specific root length (SRL: root length per unit root dry mass; Supporting Information Table S1; Liu *et al.*, 2015; Chen *et al.*, 2016; Ma *et al.*, 2018). For example, absorptive root diameter can vary over 100-fold across species (Zhang *et al.*, 2024), all else being equal, leading to a four-magnitude higher root foraging capacity as indicated by total root length for thinner roots at a given amount of root biomass. Consequently, plant species with thin and high SRL roots tend to forage for more nutrients directly through their roots, whereas species with thick absorptive roots usually rely on symbiotic mycorrhizal fungi to complement nutrient foraging (Table S1; Chen *et al.*, 2016; Ma *et al.*, 2018; Bergmann *et al.*, 2020; Matthus *et al.*, 2025). Second, upon interception, nutrients are transported across the root cortex to the stele, that is, root uptake (Ding *et al.*, 2023; Zhang *et al.*, 2023; Zhao *et al.*, 2024). Root nutrient uptake typically depends on energy from root respiration to drive the active transport of nutrients across the cortex (Table S1; George *et al.*, 2003; Hirano *et al.*, 2022), which depends on root nitrogen (N) concentration

(Tjoelker *et al.*, 2005; Reich *et al.*, 2008; Han & Zhu, 2021). Third, roots can mine nutrients via exudation of organic acids and acid phosphatases to mobilize insoluble nutrients (Table S1; Bagayoko *et al.*, 2000; Williams & de Vries, 2020; Dijkstra *et al.*, 2021; Wen *et al.*, 2022; Aoyagi *et al.*, 2025). High rates of root exudation tend to enhance nutrient availability in the rhizosphere (Bagayoko *et al.*, 2000; Williams & de Vries, 2020; Dijkstra *et al.*, 2021), which could be critical in alpine ecosystems, where most nutrients are locked in organic detritus (Chapin, 1980).

These functional processes are closely linked to the root's anatomical construction (Guo *et al.*, 2008; Lynch *et al.*, 2021). For example, absorptive root diameter, a key trait for root foraging capacity, is closely related to cortical cell size and number (Zheng *et al.*, 2024a), which in turn determine the acquisition of nutrients by roots (Lynch *et al.*, 2021). In the phloem, sieve tubes function as the conduits specialized for C transport from leaves to plant belowground tissues to support root activities like respiration and exudation (Hill *et al.*, 2007; Savage *et al.*, 2016; Hardtke, 2023), thus linking root anatomy to the uptake and mining of nutrients by roots. Root respiration and exudation rates are thus dependent on C import (Högberg *et al.*, 2001; Dilkes *et al.*, 2004; Chen *et al.*, 2025). Root respiration (reflecting root uptake) predominantly occurs in the root cortex (Lynch *et al.*, 2021), and a considerable portion of root exudates (reflecting root mining) arises from respiratory metabolites (Ryan *et al.*, 2001; Weston *et al.*, 2012). Indeed, specific root respiration declines with increasing root order, largely due to a reduction in the ratio of cortex : stele (Xia *et al.*, 2010; Jia *et al.*, 2013). Moreover, respiratory intermediates in root cortical cells act as direct precursors for the synthesis and secretion of root exudates (Johnson *et al.*, 1996; Kochian *et al.*, 2015). Therefore, unravelling how stele (e.g. sieve tube size and number) and cortical traits (e.g. cell size, number, and wall thickness) vary across plant species can offer novel insights into mechanisms underlying strategies associated with nutrient acquisition by plants.

These mechanisms responsible for variations of root traits and nutrient uptake, as well as the relationships between root traits and nutrient uptake, may be mediated by resources in the environment. Particularly, when C supply is sufficient to meet the demand for C consumption of root respiration and exudation, an increase in root respiration rate can provide more energy to drive higher exudation rates (Ataka *et al.*, 2020; Sun *et al.*, 2021; Marcellus *et al.*, 2024). Conversely, under limited C supply, more respiration could divert C away from root exudates, thereby lowering the root exudation rate (Hill *et al.*, 2007; de Vries *et al.*, 2019; Zheng *et al.*, 2024b). Notably, under severe C limitation, both root respiration and exudation may decline (Fuchslueger *et al.*, 2014; Hasibeder *et al.*, 2015). Additionally, C limitation also affects root elongation, namely root foraging (Kircher & Schopfer, 2012; Pasternak *et al.*, 2023).

Compared with leaves, our knowledge of the patterns and mechanisms underlying interspecific variations in absorptive root traits remains limited, especially in high-altitude regions (Iversen *et al.*, 2015). The unique environmental conditions in high-altitude regions, such as low temperature and low tissue decay, likely lead to root form and function that diverge from those in low-altitude regions (Iversen *et al.*, 2015; Laughlin *et al.*, 2021). For instance, our recent study has demonstrated that two key root trait components, cortex and stele, vary independently among plant species on the Tibetan Plateau (Zheng *et al.*, 2024b), whereas they are typically coupled in other ecosystems elsewhere (Kong *et al.*, 2014; Zhou *et al.*, 2018; Zhang *et al.*, 2023). Roots in the high-altitude environments also tend to exhibit larger diameters, lower SRL, and lower root tissue density (RTD, root dry mass per unit root volume) (Zadworny *et al.*, 2016, 2017), and maintain greater potential absorptive capacity per gram of fine roots across all root orders (Zadworny *et al.*, 2016). Particularly, stele tissues of absorptive roots increase at a faster rate with increasing root diameter in high-altitude environments than in low-altitude environments (X. Wang *et al.*, 2024). Additionally, in high-altitude environments, alpine plants preferably synthesize considerable secondary metabolites such as flavonoids and prolines (Ma *et al.*, 2015; Zhao *et al.*, 2019), which may lead to a reduction in soluble C allocation to root metabolic processes and soil organisms (e.g. the soil microbiome) (Körner, 2003; Chen *et al.*, 2022).

Plateau vegetation, particularly the belowground plant traits and functioning, has been poorly documented due to its relatively remote locations and low accessibility (Iversen *et al.*, 2015). Yet, plateau ecosystems are widespread around the world, pose distinct challenges to plant survival (e.g. C limitation), and harbor plant species with unique evolutionary histories and ecological strategies (Ding *et al.*, 2020; Wu *et al.*, 2022). As such, these species may have evolved distinct root strategies not captured by current global frameworks of root form and function. Additionally, because high-altitude plateaus are highly sensitive to climate change (Iversen *et al.*, 2015; Chen *et al.*, 2022), understanding the root traits of their plant communities is critical for predicting ecosystem responses to future environmental change. In this study, we measured the root traits of a wide range of common herbaceous species on the Tibetan Plateau, with a particular focus on anatomical traits and three suites of traits related to nutrient foraging, uptake, and mining. We hypothesized: (1) due to C limitation imposed by high-altitude conditions, specific root respiration and root exudation rate should be significantly correlated with root stele anatomy that governs C supply for root activities. By contrast, these root activities would not be correlated with the cortical traits. (2) In other regions globally, where limitation of nutrients rather than C dominates (Chapin, 1980), specific root respiration and root exudation rate should be coordinated with the traits associated with root foraging for efficient nutrient acquisition.

Materials and Methods

Study site

The study site is situated in the alpine meadow–steppe ecotone in the northeastern Tibetan Plateau, specifically at Haiyan Pasture (36°56′N, 101°03′E; 3200 m elevation), Haiyan County,

Qinghai Province, China. The region has a monsoon continental climate, with long, cold winters and short, cool summers. The mean annual maximum temperature is 9.4°C, the mean annual minimum temperature is −6.2°C, and the mean annual precipitation is 404 mm (based on data from 1981 to 2010) (Fig. S1). Soils are classified as Haplic Calcisols according to the FAO classification system. Alpine plant species, such as *Stipa purpurea* Griseb. (Poaceae), *Elymus nutans* Griseb. (Poaceae), *Argentina anserina* (L.) Rydb. (Rosaceae), *Allium cyaneum* Regel. (Amaryllidaceae), and *Gentiana tubiflora* (Wall. ex G. Don) Griseb. (Gentianaceae) dominate the native vegetation.

Root sampling collection and preliminary processing

This study included 42 common species, representing a diverse array of taxa in the alpine meadow–steppe ecotone (Fig. S2). These species were randomly sampled within an *c.* 40-ha experimental plot. The plot is typically grazed by yak and sheep during winter but left to grow naturally without any disturbance during summer. Root samples were collected in August 2023 during the peak of the growing season.

Root systems of individual plants were randomly sampled, following Zhou *et al.* (2022). Because plants were patchily distributed, sampling focused on high-density stands of the target species to increase the efficiency of absorptive root collection. For each species, at least 30 individuals were randomly sampled from plots that were separated by at least 20 m from each other. Soil blocks containing target plants were excavated using a pickaxe or spade, then gently compressed to loosen the soil. Root systems were exposed by carefully removing surrounding soil with forceps, sharpened needles, and brushes. Individual roots were traced to their parent plants for accurate identification.

Entire root systems or branches were categorized in the field using a stream-ordering classification system (Fig. S3a–f). Absorptive roots were defined as first- and second-order roots and used for trait measurements (Zhou *et al.*, 2021). A subset of these absorptive roots was immediately preserved for anatomical analyses by immersing them in fixing solution (formalin–aceto–alcohol solution: 90 ml of 50% ethanol, 5 ml of 100% glacial acetic acid, and 5 ml of 37% methanol), transported to the laboratory, and stored at 4°C until further analysis. Additional samples were used for root respiration measurements.

Measurements of root respiration rate

To enable timely physiological measurements, all root physiological traits were analyzed in a local temporary lab. After root categorization, absorptive roots were immediately placed into 0.9% saline solution and wrapped with moist tissue paper to prevent root system desiccation, and excess water was removed. Root respiration of absorptive roots (first- and second-order roots) was measured within 2 h of collection using an LI-6400 XT portable photosynthesis system (Li-Cor, Lincoln, NE, USA) equipped with a custom-made closed chamber (opaque PVC cylinder, 3 cm diameter, 18.5 cm length; Zheng *et al.*, 2024b). To ensure airtight gas exchange, the reference tube was sealed with plastic film. Root respiration measurements were conducted at a constant temperature of 20°C using a water bath. The sampled roots were placed into the self-made chamber, and the CO_2 mole fraction within the chamber was set to match the ambient atmospheric CO_2 concentration. To minimize artifacts caused by opening and closing the chamber, data logging began only after CO_2 concentrations in the respiration chamber stabilized, with values recorded every 5 s. For each species, four independent measurements of root respiration were obtained on sunny days between 08:30 and 16:30 h in August 2023. Root respiration rate was expressed as CO_2 afflux per unit root dry mass and time, namely, specific root respiration (nmol g^{-1} s^{-1}).

Determinations of root morphological and chemical traits

After measurements of root respiration, the root samples were immediately spread on a flatbed scanner (Epson Perfection V850 Scanner; Epson America, Long Beach, CA, USA) and scanned at 600 dpi in grayscale. Scanned images were analyzed using WinRHIZO software (v2012b; Regent Instruments Inc., Québec, QC, Canada) to obtain mean root diameter, total root length, and root volume. The scanned roots were then placed into centrifuge tubes and oven-dried at 60°C for 3 d before weighing. SRL was calculated as the ratio of total root length to dry mass. RTD was determined as the ratio of root dry mass to volume. Finally, dried root samples were ground into a fine powder using a mixer mill, and root N concentration was determined using an elemental analyzer (Vario EL III; Elementar, Hanau, Germany).

Determinations of root exudation rate and acid phosphatase activity

Root exudates were collected *in situ* from the same plants used for other root samples, following the protocol described by Phillips *et al.* (2008). Briefly, for each plant, lateral roots were carefully traced out from the plant and gently rinsed off with deionized water to remove adhering soil. Terminal (first- and second-order) roots were placed in 20 ml centrifuge tubes to collect exudates, alongside blank controls (root-free tubes). Tubes were secured in the soil and sealed with parafilm. Subsequently, a C-free nutrient solution (0.5 mM NH_4NO_3, 0.1 mM KH_2PO_4, 0.2 mM K_2SO_4, 0.15 mM $MgSO_4$, and 0.3 mM $CaCl_2$) was injected into the centrifuge tubes to provide essential mineral nutrients for root uptake. All tubes containing plant roots were covered with tinfoil to exclude light and ensure proper exudate collection. Roots inside centrifuge tubes were immediately removed after 24 h of collection, dried in an oven at 60°C for 3 d, and then weighed. The remaining solution in the centrifuge tube was filtered using a 0.22-μm filter. Then, two drops of concentrated phosphoric acid were added to the filtered solution to inhibit microbial activity, and the filtered solution was stored at −20°C until analysis of total organic C concentration, which was performed using a TOC analyzer (multi N/C 3100; Analytik, Jena, Germany).

Root acid phosphatase activity was determined following Alvey *et al.* (2001). Briefly, root samples were rinsed twice with distilled

water (5 min each) to remove extracellular acid phosphatases released from wounded cells and then placed in a 5-ml centrifuge tube. Each tube received 1.0 ml distilled water, 0.8 ml sodium acetate buffer (pH 5.8), and 0.2 ml *p*-nitrophenylphosphate substrate solution. Tubes were wrapped in aluminum foil and incubated at 20°C for 2 h. Reactions were terminated with 2 M NaOH, and absorbance was measured at 405 nm using a UV mini-1280 spectrophotometer (Shimadzu Co., Kyoto, Japan). Finally, root samples were oven-dried at 60°C for 3 d and weighed.

Measurements of root anatomical traits

Root anatomical traits were determined from FAA-preserved root samples using histological methods under light microscopy, primarily involving tissue fixation, softening, staining, dehydration, embedding, sectioning, and imaging. Specifically, 10 first- and second-order root segments with intact branching were randomly selected. These root segments were rinsed three times with deionized water to remove FAA and then soaked in a 12% hydrofluoric acid solution for 64 h to soften the tissues. Softened roots were subsequently stained with 1% safranine O, which contrasts sharply with the white paraplast wax (Freschet *et al.*, 2021). Following staining, the roots underwent dehydration through an ethanol series: 70% ethanol for 1.5 h, 80% ethanol overnight, 95% ethanol for 2 h, and three changes of 100% ethanol for 2 h. Dehydrated samples were treated in a 1 : 1 (v/v) mixture of xylene and ethanol for 1 h, followed by an additional 1-h treatment in 100% xylene.

Subsequently, roots were embedded in paraplast wax and sectioned at 10 μm thickness using a microtome (Leica RM2255; Leica Mikrosysteme Vertrieb GmbH, Bensheim, Germany). The prepared sections were stained with 0.1% Fast Green, which colors root cortex tissues green. The stained sections were then imaged using a compound microscope (DM3000; Leica). Root anatomical traits, including absorptive root cortex thickness, cortex cell size, cortex cell layer number, cortex cell wall thickness, stele diameter, vessel size, vessel number, and vessel wall thickness, were measured using ImageJ (v.1.8.0; Schneider *et al.*, 2012). Cortex cell diameter (cortex cell size), stele diameter, and vessel diameter (vessel size) were measured assuming cylindrical geometry. Cortex thickness was defined as the thickness of the cortex cell layer extending from the stele boundary to the epidermis. Cortex cell layer number refers to the number of cortex cells along a radial transect (Freschet *et al.*, 2021). Vessel number was counted per stele cross-section. Notably, due to challenges in distinguishing phloem from the stelar area under light microscopy, phloem area was not subtracted from the stele area during measurements (Freschet *et al.*, 2021; Kong *et al.*, 2021).

Determinations of root mycorrhizal colonization intensity

Arbuscular mycorrhizal (AM) colonization is closely associated with root cortex thickness (Ma *et al.*, 2018; Bergmann *et al.*, 2020). We quantified the intensity of AM colonization using standard clearing, acidifying, staining, destaining, and microscopic procedures. For each plant, at least 30 root segments from the first- and second-order roots were selected. Segments were cleared using a 10% sodium hydroxide solution (w/v) at 60°C in a water bath for 2 h. Then, the acidified root samples were immediately stained overnight at ambient temperature with 0.05% (w/v) trypan blue. Following staining, the roots were rinsed again with deionized water and incubated in a destaining solution (lactic acid : glycerin : water = 1 : 1 : 1) for several weeks. Finally, the segments were mounted on microscope slides, gently flattened, and sealed with neutral balsam. AM colonization was quantified under ×100 magnification using the cross-intersection method of McGonigle *et al.* (1990), based on at least 150 randomly selected, nonoverlapping microscopic fields per individual.

Data analysis

First, to assess trait variation across plant species, we calculated the mean, maximum, median, minimum, and coefficient of variation (CV) of each root trait. The means of each trait for each species were then used in subsequent analyses. Second, we evaluated the influence of plant phylogeny on the variation of each trait across plant species using Blomberg's *K*, where a significant *K* value indicates evolutionary conservation of traits within phylogenetic lineages (Blomberg *et al.*, 2003). Third, bivariate correlations among traits were conducted using Pearson's correlation. To further assess the strength of associations among traits after accounting for the effects of plant phylogeny, phylogenetic generalized linear models were used (Ives & Helmus, 2011). Finally, principal component analysis (PCA) was conducted to examine the multidimensional root trait covariations using the FACTOMINER package. Before PCA and correlation analyses, all data were transformed using the BESTNORMALIZE package. The package conducts a series of normalizing transformations and then selects the optimal one based on the lowest Pearson *P* test statistic for normality (Peterson, 2021). All statistical analyses were conducted in R (v.4.2.1; R Core Team, 2023).

Global data synthesis and analysis

A literature search was conducted using the Web of Science and China National Knowledge Infrastructure databases to identify studies that defined absorptive roots based on root-order classification rather than root diameter. In these selected studies, absorptive roots were considered as the first two root orders for herbaceous species and the first three root orders for woody species, respectively. From each study, we extracted those root trait values, including specific root respiration, root exudation rate, root acid phosphatase activity, root diameter, SRL, RTD, and root N concentration. Bivariate trait pairs were collected accordingly. These included 212 pairs of specific root respiration and root diameter, 211 pairs of specific root respiration and SRL, 210 pairs of specific root respiration and RTD, 202 pairs of specific root respiration and root N concentration, 61 pairs of root exudation rate and root diameter, 61 pairs of root exudation rate and SRL, 61 pairs of root exudation rate and RTD, 327 pairs of root

acid phosphatase activity and root diameter, 353 pairs of root acid phosphatase activity and SRL, and 290 pairs of root acid phosphatase activity and RTD. Notably, the global dataset did not include root physiological trait data from the Tibetan Plateau due to a lack of reports on the physiological traits of absorptive roots in the region.

Our synthesis primarily focused on herbaceous plants, while relationships between root physiological and morphological traits of woody species are provided in the Supporting Information. For herbaceous plants, the number of trait pairs ranged from zero (e.g. between acid phosphatase activity and root N concentration, acid phosphatase activity and RTD, root exudation rate and root N concentration, and root exudation rate and acid phosphatase activity) to a maximum of 142 (between root diameter and SRL). Among all traits, the most frequently reported were root diameter (n = 142) and SRL (n = 142), RTD (n = 97), followed by specific root respiration (n = 97), root exudation rate (n = 31), and root acid phosphatase activity (n = 16; Table S2).

We used simple ordinary least squares regression analyses to assess bivariate relationships among these root traits both at the global level (literature-derived) and on the Tibetan Plateau (field-collected). To test for differences in these relationships between the Tibetan Plateau and global datasets, we included interaction terms in the regression models. All data were transformed to meet normality assumptions using the BESTNORMALIZE package, while regression plots are shown using raw data for ease of interpretation.

Results

Root trait variation

We observed substantial interspecific variations in root physiological traits and mycorrhizal colonization intensity (CV: 58.0–75.8%), which were higher than those of other root traits (CV: 14.3–50.1%) across 42 co-occurring herbaceous species (Table 1). For example, root exudation rate and specific root respiration exhibited a CV of 75.8% and 64.8%, respectively (Table 1). By contrast, traits such as cortex cell wall thickness and vessel wall thickness had the least variation among all root traits, with CV values of 14.3% and 15.2%, respectively (Table 1). Further, several root traits, such as root N concentration, root diameter, stele diameter, cortex thickness, cortex cell layer number, cortex cell size, vessel wall thickness, AM colonization intensity, and specific root respiration, exhibited significant phylogenetic signals (Table 1). Notably, observed variation (CV: 39.0%) in RTD across species was threefold higher than that predicted by root structural allometry alone (CV: 10.6%, Table S3; Fig. S4).

Correlations among root traits

Root diameter was positively correlated with most root anatomical traits, such as stele diameter (r = 0.61, P < 0.001), cortex thickness (r = 0.85, P < 0.001), cortex cell layer number (r = 0.72, P < 0.001), cortex cell size (r = 0.53, P < 0.001), vessel number (r = 0.45, P = 0.002), vessel size (r = 0.36, P = 0.02), and vessel wall thickness (r = 0.36, P = 0.02; Table 2). By contrast, root diameter exhibited significant negative correlations with RTD (r = −0.65, P < 0.001) and SRL (r = −0.85, P < 0.001; Table 2). Notably, root cortex thickness increased at a faster rate than stele radius with increasing root diameter (Fig. S4). However, we observed a decoupling between cortex and stele traits (Table 2; Figs 1, S5). Cortex thickness strongly covaried with both cortex cell layer number (r = 0.92, P < 0.001) and cortex cell size (r = 0.65, P < 0.001; Table 2). Additionally, RTD was negatively correlated with cortex thickness (r = −0.58, P < 0.001), cortex cell size (r = −0.40, P = 0.008), and cortex cell layer number (r = −0.43, P = 0.005), but no significant correlation was observed between

Table 1 Summary of absorptive root traits and phylogenetic signals (Blomberg's K and P value) for 42 herbaceous species.

Root traits	Abbreviation	Mean	Median	Max	Min	CV (%)	K value	P value
Specific root length (m g^{-1})	SRL	155.45	151.09	261.34	53.72	34.24	0.23	0.41
Root tissue density (g cm^{-3})	RTD	0.34	0.35	0.64	0.09	39.02	0.22	0.50
Root N concentration (mg g^{-1})	RN	14.09	13.93	21.82	5.86	29.42	0.39	0.01
Root diameter (μm)	RD	183.72	174.87	346.88	79.19	32.93	0.37	0.008
Stele diameter (μm)	SD	63.89	59.90	119.65	20.05	44.05	0.34	0.03
Cortex thickness (μm)	CT	59.58	56.80	125.53	14.85	42.10	0.42	0.003
Cortex cell layer number	CCLN	4.55	4.30	7.00	2.08	26.41	0.38	0.01
Cortex cell size (μm)	CCS	12.43	12.62	16.97	7.60	20.33	0.33	0.05
Cortex cell wall thickness (μm)	CCWT	0.42	0.41	0.54	0.33	14.25	0.21	0.55
Vessel number	VN	6.72	5.50	14.25	2.10	50.10	0.31	0.08
Vessel size (μm)	VS	8.48	7.81	16.28	3.12	38.95	0.50	0.11
Vessel wall thickness (μm)	VWT	0.85	0.87	1.13	0.54	15.18	0.37	0.02
Root exudation rate (mg g^{-1} h^{-1})	Exud	2.60	2.18	10.33	0.60	75.83	0.26	0.22
Acid phosphatase activity (μmol g^{-1} h^{-1})	Apase	4.63	4.09	10.58	0.84	57.98	0.22	0.60
Mycorrhizal colonization intensity (%)	MCI	38.87	37.92	87.50	0.00	59.94	0.40	0.006
Specific root respiration (nmol g^{-1} s^{-1})	SRR	12.46	9.78	32.96	3.69	64.78	0.42	0.002

CV indicates the coefficient of variation of the traits across species. Max indicates the maximum value of the traits across the species. Min indicates the minimum value of the traits across the species.

New Phytologist (2025)
www.newphytologist.com

Table 2 Coefficients of Pearson's correlation for pairwise traits (upper-right diagonal with gray shading) and phylogenetic generalized linear models (lower-left diagonal with white shading; see Table 1 for abbreviations of parameters).

	SRL	RTD	RN	RD	SD	CT	CCLN	CCS	CCWT	VN	VS	VWT	Exud	Apase	MCI	SRR
SRL		0.32*	−0.08	−0.85***	−0.50***	−0.75***	−0.65***	−0.44**	−0.15	−0.39*	−0.25	−0.30*	−0.41**	−0.34*	−0.69***	−0.20
RTD	0.24		−0.17	−0.65***	−0.30*	−0.58***	−0.43**	−0.40**	−0.24	−0.12	−0.23	−0.12	−0.39**	−0.38*	−0.24	−0.36*
RN	0.00	−0.15		0.14	0.29*	0.002	−0.11	−0.14	0.15	0.23	0.51***	0.31*	0.18	0.25	0.21	0.61***
RD	−0.84***	−0.64**	0.00		0.61***	0.85***	0.72***	0.53***	0.21	0.45**	0.36*	0.36*	0.51***	0.48**	0.63***	0.36*
SD	−0.45**	−0.26*	0.00	0.64***		0.12	−0.01	0.02	0.10	0.88***	0.80***	0.67***	−0.03	0.007	0.15	0.47**
CT	−0.65***	−0.56***	0.00	0.86***	0.03		0.92***	0.65***	0.22	0.003	−0.09	0.008	0.62***	0.58***	0.72***	0.14
CCLN	−0.65***	−0.40**	0.00	0.71***	0.00	0.82***		0.42**	0.13	−0.02	−0.23	−0.13	0.58***	0.55***	0.58***	0.11
CCS	−0.49***	−0.37**	0.00	0.57***	0.08	0.61***	0.34*		0.18	−0.21	−0.05	0.08	0.22	0.23	0.46**	−0.14
CCWT	−0.10	−0.33*	0.12	0.27*	0.00	0.28*	0.14	0.12		−0.07	0.15	0.38*	0.18	0.36*	0.24	0.13
VN	−0.32*	0.00	0.00	0.42**	0.86***	0.00	0.00	0.00	0.00		0.62***	0.53***	−0.03	−0.06	0.03	0.36*
VS	−0.09	−0.18	0.42**	0.27*	0.80***	0.00	0.15	0.00	0.00	0.55***		0.69***	−0.04	0.03	0.06	0.66***
VWT	−0.20	0.00	0.14	0.28*	0.61**	0.00	0.00	0.18	0.35*	0.43**	0.61***		0.11	0.15	0.12	0.38*
Exud	−0.37**	−0.37**	0.21	0.44**	0.00	0.57***	0.56***	0.00	0.08	0.00	0.00	0.00		0.74***	0.46**	0.20
Apase	−0.27*	−0.35**	0.26*	0.39**	0.00	0.27	0.52***	0.15	0.32*	−0.10	0.00	0.00	0.75***		0.48**	0.25
MCI	−0.67***	−0.16	0.10	0.56***	0.00	0.68***	0.53***	0.43**	0.18	0.00	0.00	0.00	0.00	0.46**		0.17
SRR	0.00	−0.33*	0.55***	0.21	0.31*	0.00	0.00	0.00	0.00	0.12	0.56***	0.20	0.08	0.19	0.00	

Apase, acid phosphatase activity; CCLN, cortex cell layer number; CCS, cortex cell size; CCWT, cortex cell wall thickness; CT, cortex thickness; Exud, root exudation rate; MCI, mycorrhizal colonization intensity; RD, root diameter; RN, root N concentration; RTD, root tissue density; SD, stele diameter; SRL, specific root length; SRR, specific root respiration; VN, vessel number; VS, vessel size; VWT, vessel wall thickness.
*, $P < 0.05$; **, $P < 0.01$; ***, $P < 0.001$.

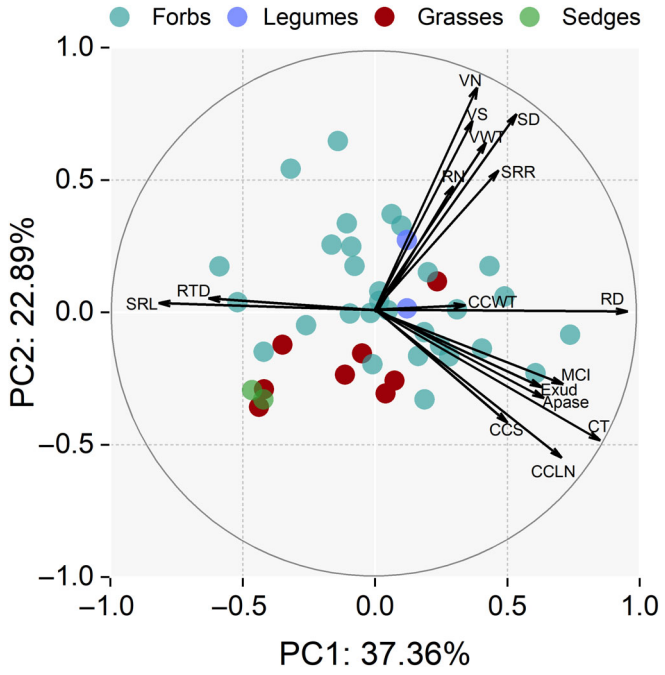

Fig. 1 Principal component analyses of absorptive root traits in an alpine meadow–steppe ecotone of the Tibetan Plateau. Apase, acid phosphatase activity; CCLN, cortex cell layer number; CCS, cortex cell size; CCWT, cortex cell wall thickness; CT, cortex thickness; Exud, root exudation rate; MCI, mycorrhizal colonization intensity; RD, root diameter; RN, root N concentration; RTD, root tissue density; SD, stele diameter; SRL, specific root length; SRR, specific root respiration; VN, vessel number; VS, vessel size; VWT, vessel wall thickness.

RTD and cortex cell wall thickness or between RTD and stele traits (Table 2). Phylogenetic signal exerted minimal influence on these inter-trait relationships (Table 2).

Multivariate ordination analysis

PCA and pPCA revealed similar patterns of variation in absorptive root traits on the Tibetan Plateau (Figs 1, S5). PCA revealed that the first two principal components (PC1 and PC2) collectively accounted for 60.25% of the total variation in root traits, with PC1 contributing 37.36% and PC2 contributing 22.89% (Fig. 1; Table S4). PC1 predominantly captured coordinated variation between nutrient-foraging strategies (SRL, AM colonization intensity, and root diameter), nutrient-mining strategies (root exudation rate and root acid phosphatase activity), and among cortex traits (cortex thickness, cortex cell size, cortex cell layer number, and cell wall thickness). SRL was significantly and negatively correlated with cortical traits, such as cortex thickness ($r = -0.75$, $P < 0.001$), cortex cell size ($r = -0.44$, $P = 0.004$), and cortex cell layer number ($r = -0.65$, $P < 0.001$). By contrast, AM colonization intensity was significantly and positively correlated with cortex thickness ($r = 0.72$, $P < 0.001$), cortex cell size ($r = 0.46$, $P = 0.002$), and cortex cell layer number ($r = 0.58$, $P < 0.001$; Table 2). Like AM colonization intensity, both root exudation rates and acid phosphatase activities were correlated with cortex-related traits (e.g. cortex thickness and cortex cell layer number), but not stele traits (Table 2).

PC2 integrated co-variation patterns between nutrient uptake strategies (specific root respiration) and root stele morphology and anatomy (e.g. stele diameter, vessel diameter, and vessel density). Specific root respiration was positively correlated with stele diameter ($r = 0.47$, $P = 0.002$), vessel size ($r = 0.66$, $P < 0.001$), vessel number ($r = 0.36$, $P = 0.02$), and vessel wall thickness ($r = 0.38$, $P = 0.01$), but not correlated with cortex traits (Table 2). Importantly, the PCA illustrated that both nutrient-mining strategies and AM foraging strategies were closely linked to cortex traits and decoupled from stele traits. Conversely, nutrient-uptake strategies exhibited strong linkages with stele traits but were decoupled from cortex traits (Figs 1, S5).

Nutrient acquisition strategies for Tibetan Plateau plants compared with global patterns

Specific root respiration from plants growing on the Tibetan Plateau was positively correlated with root diameter and root N concentration and negatively correlated with RTD but showed no relationship with SRL (Table 2; Fig. 2a–d). By contrast, in other regions of the world, specific root respiration was positively correlated with SRL and had no relationship with root diameter (Figs 2a,b, S6a,b). Moreover, the root exudation rate of plant species on the Tibetan Plateau was positively correlated with root diameter and negatively correlated with both SRL and RTD (Table 2; Fig. 3a–c). By contrast, for the global sample of plants, the root exudation rate was positively correlated with SRL, while the root exudation rate was not correlated with root diameter at the other regions globally (Figs 3a,b, S7a,b). Additionally, root acid phosphatase activity was consistently and positively correlated with root diameter and negatively correlated with SRL in both Tibetan Plateau plants and global plant samples (Table 2; Figs 4a,b, S8a,b). Notably, for plant species on the Tibetan Plateau, root acid phosphatase activity was negatively correlated with RTD, while no such relationship was observed in global woody plant datasets (Table 2; Figs 4c, S8c).

Discussion

We discovered unique coordination between root structural and functional traits among herbaceous plants in alpine grasslands of the Tibetan Plateau. Specifically, specific root respiration, a key indicator of root metabolic activity including active nutrient uptake, was tightly coupled with root vascular traits. This supports our Hypothesis 1 that absorptive root respiration would be significantly correlated with the root stele traits that govern C supply for root activities due to C limitations imposed by high-altitude conditions. However, root exudation rates and acid phosphatase activity, which reflect the root system's capacity to mine soil nutrients, were associated with cortex traits. This is inconsistent with our Hypothesis 1, which states that the absorptive root exudation rate would be significantly correlated with root stele traits. Moreover, nutrient acquisition strategies of plants growing on the Tibetan Plateau were mostly related to

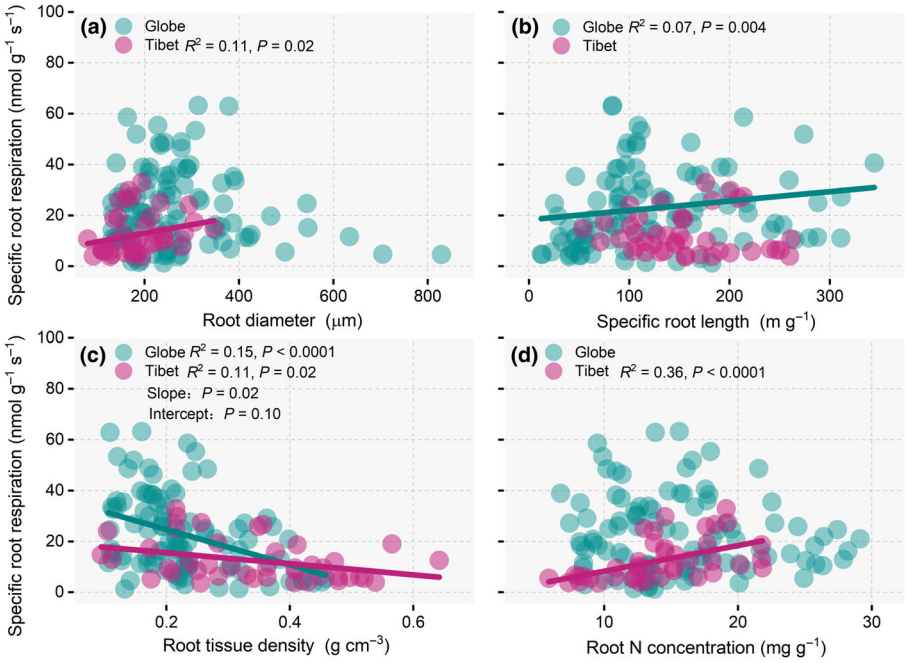

Fig. 2 Ordinary least squares regressions between specific root respiration and other root traits, including root diameter (a), specific root length (b), root tissue density (c), and root N concentration (d). Globe and Tibet indicate the literature-derived herbaceous dataset and our field-collected dataset from plants on the Tibetan Plateau, respectively.

root diameter. By contrast, SRL was closely associated with nutrient acquisition in the other regions globally. These observations are consistent with our Hypothesis 2. The unique coordination among nutrient foraging, uptake, and mining strategies of plant species on the Tibetan Plateau fundamentally sheds essential light on our understanding of the unique root form and function in plant adaptation to alpine environments.

Coupling of nutrient uptake strategies with vascular traits rather than cortex traits

We observed that root respiration rates were closely linked to root vessel morphology, underscoring the central role of the root stele in meeting metabolic demands. This pattern likely reflects the unique climatic conditions on the Tibetan Plateau, which are distinguished by low annual mean temperature below 0°C (Yuan *et al.*, 2022), hypoxic conditions with only 65% of the atmospheric oxygen content present at sea level (Liu *et al.*, 2023), and intense ultraviolet radiation comparable to equatorial regions (Gao & Zhou, 1998; Andersen *et al.*, 2016). Such extreme climates drive plants to preferentially allocate C toward the biosynthesis of secondary metabolites, such as flavonoids and proline, to cope with these environmental stresses (Ma *et al.*, 2015; Zhao *et al.*, 2019). This pattern of C allocation to defense compounds is expected to constrain respiratory substrate availability (Högberg *et al.*, 2001; Jiang *et al.*, 2023). Therefore, absorptive roots with large-sized vascular systems (e.g. enlarged sieve tube diameter and more sieve tubes) would have high transport efficiency of photosynthate to maintain root respiratory demand (Savage *et al.*, 2016; Hardtke, 2023).

Although we did not directly measure sieve tube traits due to challenges in visualizing phloem anatomy under conventional staining techniques (Evert, 2006), vessel traits may serve as reliable proxies. Sieve tubes and vessels are structurally and functionally coupled. For example, thick vessels are often accompanied by thick sieve tubes (see Schrader *et al.*, 2004; Cutler *et al.*, 2008; Hölttä *et al.*, 2009; Kong *et al.*, 2021). Thus, changes in vessel size and density in the study likely reflect an increased capacity for photosynthate transport, which in turn supports higher root respiratory activity (Hölttä *et al.*, 2009; Kong *et al.*, 2021).

Interestingly, we found that specific root respiration was decoupled from cortex anatomical traits, which may arise from offsetting effects of cortex cell size and cell number on specific root respiration. For example, when the cross-sectional area of cortex cells increases from 100 to 500 μm^2, the specific root respiration rate is reduced by *c.* 50% (Chimungu *et al.*, 2014). This is because larger cortex cells are usually associated with a larger proportion of vacuoles and a lower proportion of cytoplasm, which is the metabolically active part of root cortex cells and directly controls overall root respiration (Sidhu & Lynch, 2024). Furthermore, a greater vacuolar size in thicker cortex cells can store more secondary metabolites to resist environmental stresses (Marty, 1999; Ferreyra *et al.*, 2012; Ramakrishna *et al.*, 2025), consequently leading to less C allocation to cell respiration. Conversely, an increase in cortex cell number among cortical layers usually increases specific root respiration (Lopez-Valdivia *et al.*, 2023; Sidhu *et al.*, 2023). Although cortex cell size and cell number increase simultaneously with increasing root diameter, their opposite effects on specific root respiration may cancel each other out, thus explaining the lack of significant relationships between cortex traits (cortex thickness, cortex cell size, and cell numbers) and specific root respiration. Such a functional trade-off between root storage (or defense) and root metabolism likely underlies the divergent strategies by which alpine plants cope with the harsh environments of the Tibetan Plateau.

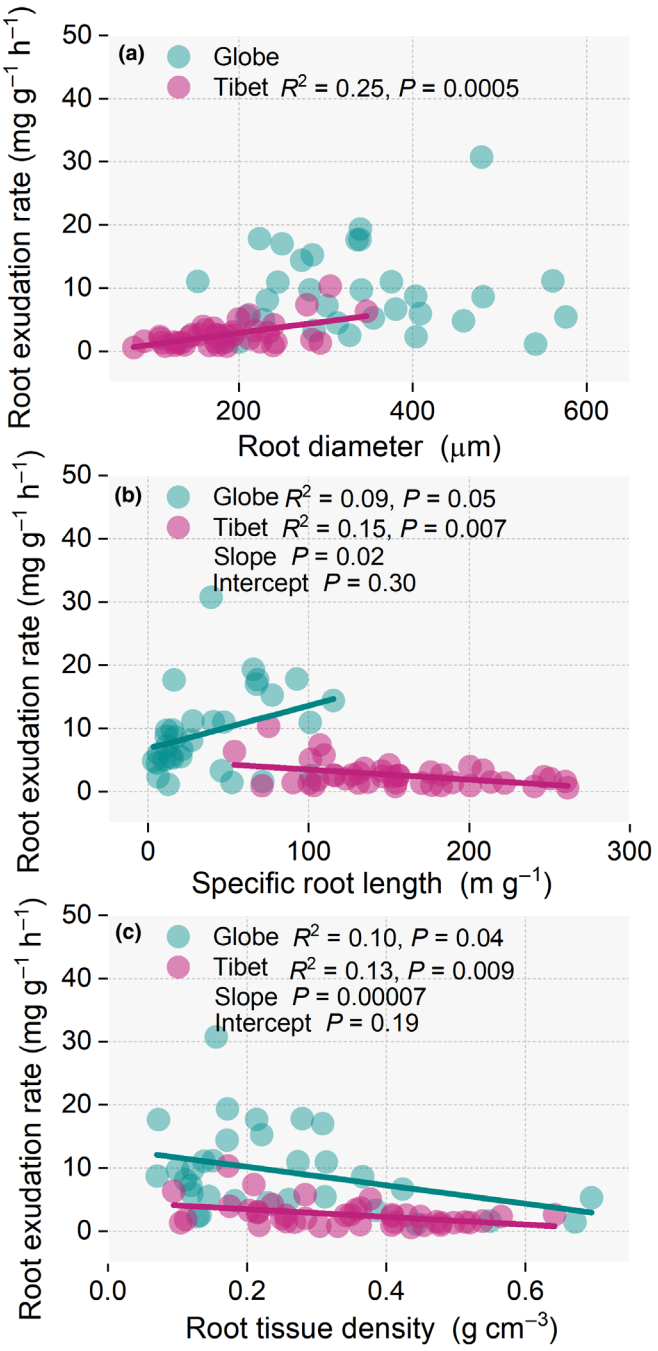

Fig. 3 Ordinary least squares regressions between absorptive root exudation rate and root morphological traits, including root diameter (a), specific root length (b), and root tissue density (c). Globe and Tibet indicate the literature-derived herbaceous dataset and our field-collected dataset from plants on the Tibetan Plateau, respectively.

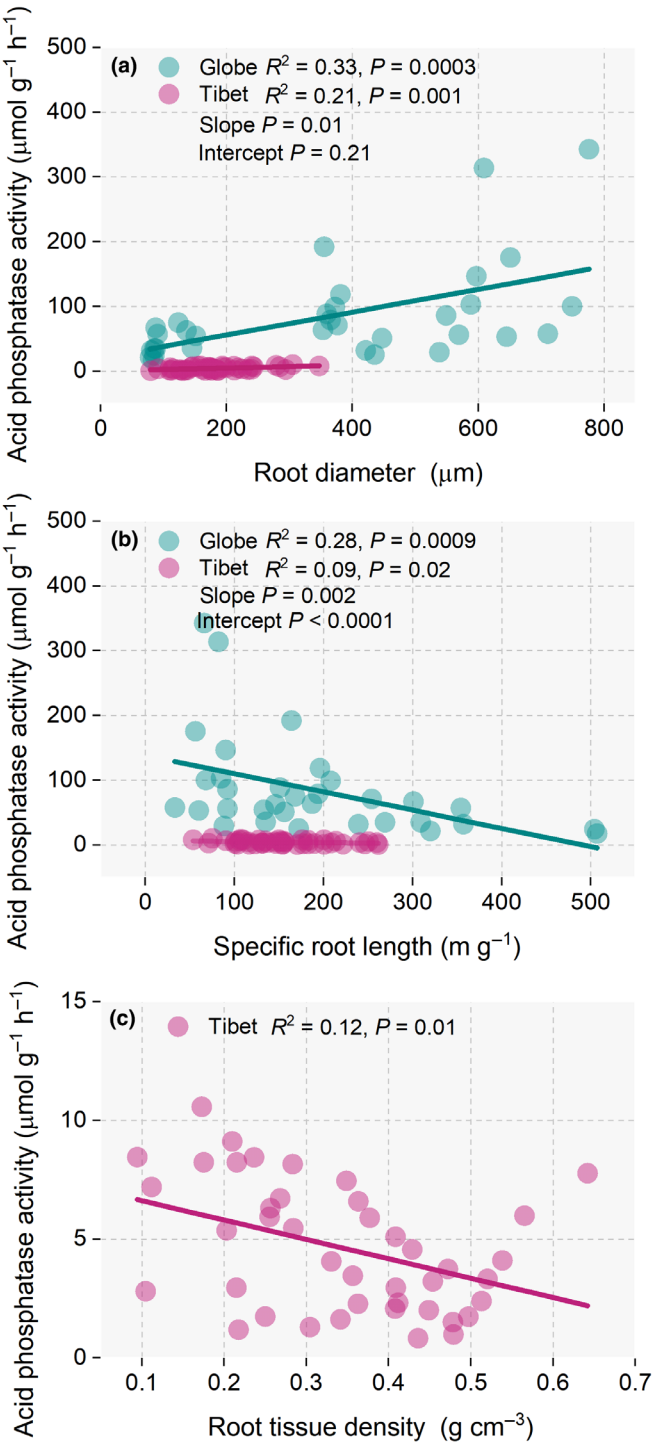

Fig. 4 Ordinary least squares regressions between acid phosphatase activity and root morphological traits, including root diameter (a), specific root length (b), and root tissue density (c). Globe and Tibet indicate the literature-derived herbaceous dataset and our field-collected dataset from plants on the Tibetan Plateau, respectively.

It should be noted that root respiration in this study likely reflected primarily maintenance costs associated with nutrient uptake and/or exudation, as roots were sampled at peak biomass when shoot and root growth had largely ceased (King *et al.*, 2002; Bai *et al.*, 2010). Although root exudation appears to incur lower energetic costs (as discussed below), future studies should disentangle the relative contributions of respiration to nutrient uptake vs exudation, for example using isotope labeling, to more fully capture how root form and function adapt to alpine conditions (Kong & Fridley, 2019).

Coupling of nutrient mining strategies with cortex traits rather than vascular traits

A key finding in this study is the negative correlation between RTD and root mining strategy, as indicated by root exudation rates and root acid phosphatase activity (Table 2). It is well established that the relative size of the cortex and stele has a substantial effect on RTD. For example, root cortex thickness increases at a much faster rate than the root stele radius with increasing root diameter, a well-known phenomenon in root structural allometry (Kong *et al.*, 2014; Zhang *et al.*, 2023, 2024). Given that root cortex typically has lower RTD than root stele, the root structural allometry would lead to lower RTD in thicker absorptive roots (Kong *et al.*, 2019; Zhang *et al.*, 2023, 2024). However, we observed that RTD was much lower than that predicted by global allometric relationships (Table S3; Fig. S4). For example, at a root diameter of 346 μm, root structural allometry predicts an RTD of 0.23 g cm^{-3}, whereas the measured RTD was only 0.09 g cm^{-3} (Table S3; Fig. S4). This discrepancy may suggest that root structural allometry alone cannot fully account for interspecific variation in RTD, as species at this alpine site strongly deviate from the expected global patterns.

Interestingly, RTD was found to be correlated with cortex cell characteristics (e.g. cell size and cell number), but not with vessel traits, that is, vessel diameter, vessel number, and vessel wall thickness (Table 2). Because both cortex cell size and layer number increased with root diameter (Table 2), we infer that the observed decrease in RTD with root diameter results not only from the root structural allometry but also from increases in cortex cell size and number. Importantly, as cortex cell volume expands, the proportion of vacuoles substantially increases, whereas the proportion of cytoplasm declines (Chimungu *et al.*, 2014; Sidhu & Lynch, 2024). Since vacuoles are primarily composed of water and contribute little to dry mass, a greater vacuolar proportion would lead to reduced RTD by lowering biomass per unit root volume.

Notably, this shift toward vacuole-dominated cortex cells tends to influence root exudation. A lower RTD reflects reduced construction costs, allowing more C to be allocated to exudates (Sun *et al.*, 2021; Williams *et al.*, 2021). Moreover, an increased proportion of vacuole volume tends to be accompanied by a greater amount of secondary metabolic products (Ferreyra *et al.*, 2012), thereby providing more substrates for exudation. Additionally, the expansion of cortex cell volume significantly increases the surface area of the endomembrane system within cortex cells. For example, emerging evidence reveals that an increase in cortex cell lumen per unit corresponds to a 0.14- and 0.86-unit increase in cytoplasmic and vacuolar lumen, respectively (Sidhu & Lynch, 2024). This expanded membrane system within cortical cells potentially provides more proteins for proton pumps and transport proteins in roots (Komis *et al.*, 2015; Vives-Peris *et al.*, 2020; Carlson *et al.*, 2024), thereby facilitating the transmembrane transport of exudates (Meyer *et al.*, 2010; Honsbein *et al.*, 2011). These results warrant the inclusion of vacuolar characteristics in cortex cells as a factor to explain root exudation rates in future studies.

Changes in cortex cell wall anatomy may also influence RTD (Lynch *et al.*, 2024; Sidhu *et al.*, 2024). For example, thicker cell walls are often associated with higher RTD (Sidhu *et al.*, 2023; Han *et al.*, 2024). However, we observed no correlation between cortex cell wall thickness and RTD in this study (Table 2). One possibility is that increases in cortex cell diameter are accompanied by compositional changes in the cortex cell wall, such as reductions in lignin and increases in pectin proportions that decrease overall RTD (Schneider *et al.*, 2021; Han *et al.*, 2024; M. Wang *et al.*, 2024; X. Wang *et al.*, 2024). These compositional shifts may also reduce resistance to the diffusion of root exudates (Akatsuki & Makita, 2020). Therefore, future work should examine how the chemical composition of cortex cell walls influences RTD and exudation, particularly in the wild plant species adapted to harsh environments.

Nutrient acquisition strategies on the Tibetan Plateau compared with other regions

On the Tibetan Plateau, root diameter was significantly and positively correlated with specific root respiration, root exudation rates, and mycorrhizal colonization intensity (Table 2; Figs 2a, 3a), indicating that root diameter is the primary trait dominating interspecific variation in nutrient acquisition strategies in this alpine ecosystem. The central role of root diameter likely stems from cellular-level differences in root tissues that simultaneously determine anatomical structure and functional capacity. For example, increased root diameter facilitates the supply of substrates for root respiration and improves active nutrient uptake by increasing tube size and number. Meanwhile, as root diameter increases, the expansion of cortex cell volume may lead to an increased proportion of vacuoles and possible alterations in cell wall composition, which promotes root exudation and enhances the ability to mine nutrients from the soil. Furthermore, thicker cortices increase the area for mycorrhizal symbiosis, thereby improving the capacity to forage for nutrients (Brundrett & Tedersoo, 2018; Ma *et al.*, 2018; Bergmann *et al.*, 2020).

In contrast to our results on the Tibetan Plateau, the global dataset from plants grown in other regions showed that SRL, rather than diameter, was more strongly linked to root nutrient foraging, uptake, and mining. Specifically, SRL was positively correlated with specific root respiration and root exudation rates (Figs 2b, 3b, S6b, S7b). This is because higher SRL reflects reduced C investment per unit root length, which is thought to be associated with increased metabolic activities (manifested as higher respiration and exudation rates) (Roumet *et al.*, 2016; Meier *et al.*, 2020; Liang *et al.*, 2023). This aligns with our observation that both root respiration and exudation rates were significantly and negatively correlated with RTD, a proxy of C investment in roots (Figs 2c, 3c). Higher SRL results in a greater root surface area per unit biomass (i.e. higher specific root area in contact with soil), thereby enhancing root intrinsic ability to forage for nutrients (Chen *et al.*, 2016; Zhang *et al.*, 2024). Thus, across global plant communities, the trade-off between root construction cost and metabolic investment likely drives the

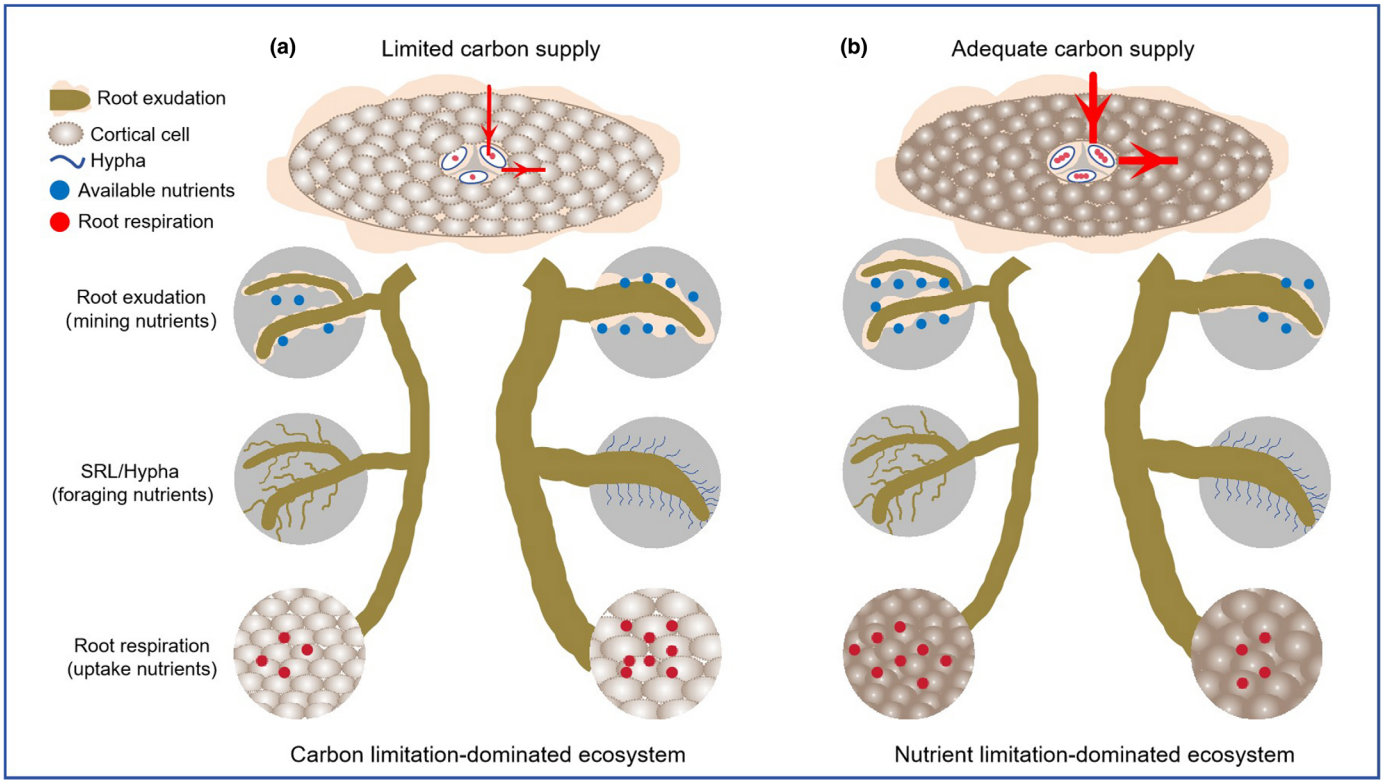

Fig. 5 Conceptual framework of nutrient acquisition strategies on the Tibetan Plateau (a) and in other global regions (b). The two main root structures depicted in panels (a, b) represent absorptive roots of contrasting diameters (thinner roots on the left vs thicker roots on the right). The cortical cells in each panel are shaded to reflect varying strengths of carbon supply from aboveground sources: panel (a) illustrates roots under low supply on the Tibetan Plateau, while panel (b) represents conditions of high carbon supply at a global scale. The arrows indicate carbon input to the roots: a large arrow indicates adequate carbon input, while a small arrow indicates limited carbon input.

coordination among nutrient foraging, uptake, and mining (Sun *et al.*, 2021; Williams *et al.*, 2021; Liang *et al.*, 2023).

Conclusions

This study reveals insights into how herbaceous plant species on the Tibetan Plateau adopt nutrient acquisition strategies that diverge markedly from global patterns. On the Tibetan Plateau, the three key processes of root nutrient acquisition – namely, foraging, uptake, and mining nutrients – are predominantly driven by cellular-level root anatomical traits. Specifically, nutrient uptake seems to be primarily mediated by vascular cell size and density. By contrast, the nutrient mining strategy is associated with cortex cell size, cell number, and cell wall composition (Fig. 5a). However, global coordination among nutrient acquisition strategies is primarily determined by trade-offs between root construction costs and metabolic activity, with SRL serving as a key mediator (Fig. 5b). The unique trait–function relationships on the Tibetan Plateau likely represent adaptive characteristics of plants to the extreme climate. Therefore, these novel findings provide fruitful insights into plant coexistence in high-altitude grasslands and can predict how alpine plant communities may respond to ongoing and future climatic changes.

Acknowledgements

We are grateful to the editor (Richard J. Norby) and three anonymous reviewers for their thoughtful comments on the first draft and also appreciate Luke McCormack's comments on the manuscript. This study was funded by the National Natural Science Foundation of China (32360252 and 32060286). DK was supported by the National Natural Science Foundation of China (32471824 and 32171746), the leading talents of basic research in Henan Province, the Excellent Youth Creative Research Group Project in Henan Province (252300421002), Foreign Scientists Studio in Henan Province (GZS2025011), and the Scientific Research Foundation of Henan Agricultural University (30500854). JW was supported by the National Natural Science Foundation of China (42122054 and 42477227), Guangdong Provincial Key Laboratory of Soil and Groundwater Pollution Control (2023B1212060002), and High-level University Special Fund (G03050K001). JD was supported by the Henan Postdoctoral Foundation.

Competing interests

None declared.

Author contributions

ZZ designed the study. ZZ, FD, ZL and LC performed the experiment. ZZ, DK and FD analyzed the data. ZZ, DK and FD wrote the first draft. All coauthors contributed to the revision.

ORCID

Junxiang Ding https://orcid.org/0000-0003-3782-9966
J. Aaron Hogan https://orcid.org/0000-0001-9806-3074
Deliang Kong https://orcid.org/0000-0002-3418-3787
Oscar J. Valverde-Barrantes https://orcid.org/0000-0002-7327-7647
Junjian Wang https://orcid.org/0000-0002-3040-0924
Monique Weemstra https://orcid.org/0000-0002-6994-2501
Wen-Hao Zhang https://orcid.org/0000-0003-2708-2221
Zhi Zheng https://orcid.org/0000-0001-9665-0179

Data availability

Data underlying this article are available at figshare: https://doi.org/10.6084/m9.figshare.30109732.v1.

References

Akatsuki M, Makita N. 2020. Influence of fine root traits on *in situ* exudation rates in four conifers from different mycorrhizal associations. *Tree Physiology* **40**: 1071–1079.

Alvey S, Bagayoko M, Neumann G, Buerkert A. 2001. Cereal/legume rotation effects in two West African soils under controlled conditions. *Plant and Soil* **231**: 45–54.

Andersen TB, Dalgaard CJ, Selaya P. 2016. Climate and the emergence of global income differences. *Review of Economic Studies* **83**: rdw006.

Aoyagi R, Kobayashi R, Turner BL. 2025. Interspecific and intraspecific variations in root phosphatase activity among tropical tree species with different soil phosphorus associations. *Journal of Ecology* **113**: 1686–1698.

Ataka M, Sun LJ, Nakaji T, Katayama A, Hiura T. 2020. Five-year nitrogen addition affects fine root exudation and its correlation with root respiration in a dominant species, *Quercus crispula*, of a cool temperate forest, Japan. *Tree Physiology* **40**: 367–376.

Bagayoko M, Alvey S, Neumann G, Buerker A. 2000. Root-induced increases in soil pH and nutrient availability to field-grown cereals and legumes on acid sandy soils of Sudano-Sahelian West Africa. *Plant and Soil* **225**: 117–127.

Bai W, Wan S, Niu S, Liu W, Chen Q, Wang Q, Zhang W, Han X, Li L. 2010. Increased temperature and precipitation interact to affect root production, mortality, and turnover in a temperate steppe: implications for ecosystem C cycling. *Global Change Biology* **16**: 1306–1316.

Bergmann J, Weigelt A, Plas F, Laughlin DC, Mommer L. 2020. The fungal collaboration gradient dominates the root economics space in plants. *Science Advances* **6**: eaba3756.

Blomberg SP, Garland JT, Ives AR. 2003. Testing for phylogenetic signal in comparative data: behavioral traits are more labile. *Evolution* **57**: 717–745.

Brundrett M, Tedersoo L. 2018. Evolutionary history of mycorrhizal symbioses and global host plant diversity. *New Phytologist* **220**: 1108–1115.

Carlson RP, Beck AE, Benitez MG, Harcombe WR, Mahadevan R, Gedeon T. 2024. Cell geometry and membrane protein crowding constrain growth rate, overflow metabolism, respiration, and maintenance energy. *bioRxiv*. doi: 10.1101/2024.08.21.609071.

Carmona CP, Bueno GB, Toussaint A, Träger S, Díaz S, Moora M, Munson AD, Pärte M, Zobel M, Tamme R. 2021. Fine-root traits in the global spectrum of plant form and function. *Nature* **597**: 683–687.

Chapin FS. 1980. The mineral nutrition of wild plants. *Annual Review of Ecology and Systematics* **11**: 233–260.

Chen H, Ju P, Zhu Q, Xu X, Wu N, Gao Y, Feng X, Tian J, Niu S, Zhang Y *et al.* 2022. Carbon and nitrogen cycling on the Qinghai-Tibetan Plateau. *Nature Reviews Earth and Environment* **3**: 701–716.

Chen J, Cao J, Guo B, Han M, Feng Z, Tang J, Mo X, Wang J, Yang Q, Pei Y *et al.* 2025. Increased dependence on mycorrhizal fungi for nutrient acquisition under carbon limitation by tree girdling. *Plant Diversity* **47**: 466–478.

Chen W, Koidea RT, Adamsa TS, DeForestd JL, Cheng L, Eissenstat DM. 2016. Root morphology and mycorrhizal symbioses together shape nutrient foraging strategies of temperate trees. *Proceedings of the National Academy of Sciences, USA* **113**: 8741–8746.

Chimungu JG, Brown KM, Lynch JP. 2014. Large root cortical cell size improves drought tolerance in maize. *Plant Physiology* **166**: 2166–2178.

Cutler DF, Botha T, Stevenson DW. 2008. *Plant anatomy: an applied approach.* Oxford, UK: Blackwell Publishing.

Díaz S, Kattge J, Cornelissen JHC, Wright IJ, Lavorel S, Dray S, Reu B, Kleyer M, Wirth C, Prentice IC *et al.* 2016. The global spectrum of plant form and function. *Nature* **529**: 167–171.

Dijkstra FA, Zhu B, Cheng W. 2021. Root effects on soil organic carbon: a double-edged sword. *New Phytologist* **230**: 60–65.

Dilkes NB, Jones DL, Farrar J. 2004. Temporal dynamics of carbon partitioning and rhizodeposition in wheat. *Plant Physiology* **134**: 706–715.

Ding J, Yin H, Kong D, Liu Q, Zhang Z, Wang Q, Guo W, Valverde-Barrantes OJ, Wang J, Liu Z. 2023. Precipitation, rather than temperature drives coordination of multidimensional root traits with ectomycorrhizal fungi in alpine coniferous forests. *Journal of Ecology* **111**: 1935–1949.

Ding WN, Ree RH, Spicer RA, Xing YW. 2020. Ancient orogenic and monsoondriven assembly of the world's richest temperate alpine flora. *Science* **369**: 578–581.

Evert RF. 2006. *Esau's plant anatomy: meristems, cells, and tissues of the plant body: their structure, function, and development.* Hoboken, NJ, USA: John Wiley & Sons.

Ferreyra MLF, Rius SP, Casati P. 2012. Flavonoids: biosynthesis, biological functions, and biotechnological applications. *Frontiers in Plant Science* **3**: 222.

Freschet GT, Pagès L, Iversen CM, Comas LH, Rewald B, Roumet C, Klimešová J, Zadworny M, Poorter H, Postma JA *et al.* 2021. A starting guide to root ecology: strengthening ecological concepts and standardising root classification, sampling, processing and trait measurements. *New Phytologist* **232**: 973–1122.

Fuchslueger L, Bahn M, Fritz K, Hasibeder R, Richter A. 2014. Experimental drought reduces the transfer of recently fixed plant carbon to soil microbes and alters the bacterial community composition in a mountain meadow. *New Phytologist* **201**: 916–927.

Gao D, Zhou L. 1998. The advance of environment meteorology on the Qinghai-Xizang Plateau. *Progress in Geophysics* **14**: 17–28.

George K, Norby RJ, Hamilton JG, DeLucia EH. 2003. Fine-root respiration in a loblolly pine and sweetgum forest growing in elevated CO_2. *New Phytologist* **160**: 511–522.

Guo D, Xia M, Wei X, Chang W, Liu Y, Wang Z. 2008. Anatomical traits associated with absorption and mycorrhizal colonization are linked to root branch order in twenty-three Chinese temperate tree species. *New Phytologist* **180**: 673–683.

Han M, Zhu B. 2021. Linking root respiration to chemistry and morphology across species. *Global Change Biology* **27**: 190–201.

Han Q, Yang Q, Guo B, Kong D. 2024. Linking root cell wall width with plant functioning under drought conditions. *Journal of Experimental Botany* **75**: 5463–5466.

Hardtke CS. 2023. Phloem development. *New Phytologist* **239**: 852–867.

Hasibeder R, Fuchslueger L, Richter A, Bahn M. 2015. Summer drought alters carbon allocation to roots and root respiration in mountain grassland. *New Phytologist* **205**: 1117–1127.

Hill P, Kuzyakov Y, Jones D, Farrar J. 2007. Response of root respiration and root exudation to alterations in root C supply and demand in wheat. *Plant and Soil* **291**: 131–141.

Hirano T, Cui R, Sun L, Teramoto M, Liang N. 2022. Partitioning of root respiration into growth, maintenance, and ion uptake components in a young larch-dominated forest. *Plant and Soil* **482**: 57–72.

Högberg P, Nordgren A, Buchmann N, Taylor AFS, Ekblad A, Högberg MN, Nyberg G, Ottosson-Löfvenius M, Read DJ. 2001. Large-scale forest girdling shows that current photosynthesis drives soil respiration. *Nature* **411**: 789–792.

Hölttä T, Mencuccini M, Nikinmaa E. 2009. Linking phloem function to structure: analysis with a coupled xylem-phloem transport model. *Journal of Theoretical Biology* **259**: 325–337.

Honsbein A, Blatt MR, Grefen C. 2011. A molecular framework for coupling cellular volume and osmotic solute transport control. *Journal of Experimental Botany* **62**: 2363–2370.

Iversen CM, Sloan VL, Sullivan PF, Euskirchen ES, McGuire AD, Norby RJ, Walker AP, Warren JM, Wullschleger SD. 2015. The unseen iceberg: plant roots in arctic tundra. *New Phytologist* **205**: 34–58.

Ives AR, Helmus MR. 2011. Generalized linear mixed models for phylogenetic analyses of community structure. *Ecological Monographs* **81**: 511–525.

Jia S, McLaughlin NB, Gu J, Li X, Wang Z. 2013. Relationships between root respiration rate and root morphology, chemistry and anatomy in *Larix gmelinii* and *Fraxinus mandshurica*. *Tree Physiology* **33**: 579–589.

Jiang Q, Jia L, Chen Y, Yang Z, Chen S, Xiong D, Liu X, Wang X, Yao X, Chen T *et al.* 2023. Substrate and adenylate limit subtropical tree fine-root respiration under soil warming. *Plant, Cell & Environment* **46**: 2827–2840.

Johnson JF, Vance CP, Allan DL. 1996. Phosphorus deficiency in *Lupinus albus*. *Plant Physiology* **112**: 31–41.

King JS, Albaugh TJ, Allen HL, Buford M, Strain BR, Dougherty P. 2002. Below-ground carbon input to soil is controlled by nutrient availability and fine root dynamics in loblolly pine. *New Phytologist* **154**: 389–398.

Kircher S, Schopfer P. 2012. Photosynthetic sucrose acts as cotyledon-derived long-distance signal to control root growth during early seedling development in *Arabidopsis*. *Proceedings of the National Academy of Sciences, USA* **109**: 11217–11221.

Kochian LV, Piñeros MA, Liu J, Magalhaes JV. 2015. Plant adaptation to acid soils: the molecular basis for crop aluminum resistance. *Annual Review of Plant Biology* **66**: 571–598.

Komis G, Šamajová O, Ovečka M, Šamaj J. 2015. Super-resolution microscopy in plant cell imaging. *Trends in Plant Science* **20**: 834–843.

Kong D, Fridley JD. 2019. Does plant biomass partitioning reflect energetic investments in carbon and nutrient foraging? *Functional Ecology* **33**: 1627–1637.

Kong D, Ma C, Zhang Q, Li L, Chen X, Zeng H, Guo D. 2014. Leading dimensions in absorptive root trait variation across 96 subtropical forest species. *New Phytologist* **203**: 863–872.

Kong D, Wang J, Valverde-Barrantes OJ, Kardol P. 2021. A framework to assess the carbon supply-consumption balance in plant roots. *New Phytologist* **229**: 659–664.

Kong D, Wang J, Wu H, Valverde-Barrantes OJ, Wang R, Zeng H, Kardol P, Zhang H, Feng Y. 2019. Nonlinearity of root trait relationships and the root economics spectrum. *Nature Communications* **10**: 1–9.

Körner C. 2003. Carbon limitation in trees. *Journal of Ecology* **91**: 4–17.

Laughlin DC, Mommer L, Sabatini FM, Bruelheide H, Kuyper TW, McCormack ML, Bergmann J, Freschet GT, Guerrero-Ramírez NR, Iversen CM *et al.* 2021. Root traits explain plant species distributions along climatic gradients yet challenge the nature of ecological trade-offs. *Nature Ecology & Evolution* **5**: 1123–1134.

Liang S, Guo H, McCormack ML, Qian Z, Huang K, Yang Y, Xi M, Qi X, Ou X, Liu Y *et al.* 2023. Positioning absorptive root respiration in the root economics space across woody and herbaceous species. *Journal of Ecology* **111**: 2710–2720.

Liu B, Li H, Zhu B, Koide RT, Eissenstat DM, Guo D. 2015. Complementarity in nutrient foraging strategies of absorptive fine roots and arbuscular mycorrhizal fungi across 14 coexisting subtropical tree species. *New Phytologist* **208**: 125–136.

Liu R, Shi P, Tang H, Wang J, Zhao C, Zhu W. 2023. Vegetation oxygen production and its contribution rate to near-surface atmospheric oxygen concentration on the Qinghai-Tibet Plateau. *Acta Geographica Sinica* **78**: 1136–1152.

Lopez-Valdivia I, Yang X, Lynch JP. 2023. Large root cortical cells and reduced cortical cell files improve growth under suboptimal nitrogen *in silico*. *Plant Physiology* **192**: 2261–2275.

Lynch JP, Galindo-Castañeda T, Schneider HM, Sidhu JS, Rangarajan H, York LM. 2024. Root phenotypes for improved nitrogen capture. *Plant and Soil* **502**: 31–85.

Lynch JP, Strock CF, Schneider HM. 2021. Root anatomy and soil resource capture. *Plant and Soil* **466**: 21–63.

Ma L, Sun X, Kong X, Galvan JV, Li X, Yang S, Yang Y, Yang Y, Hu X. 2015. Physiological, biochemical and proteomics analysis reveals the adaptation strategies of the alpine plant *Potentilla saundersiana* at altitude gradient of the Northwestern Tibetan Plateau. *Journal of Proteomics* **112**: 63–82.

Ma Z, Guo D, Xu X, Lu MZ, Bardgett RD, Eissenstat DM, McCormack ML, Hedin LO. 2018. Evolutionary history resolves global organization of root functional traits. *Nature* **555**: 94–97.

Marcellus M, Goud EM, Swartz N, Brown E, Soper FM. 2024. Evolutionary history and root trait coordination predict nutrient strategy in tropical legume trees. *New Phytologist* **243**: 1711–1723.

Marty F. 1999. Plant vacuoles. *Plant Cell* **11**: 587–599.

Matthus M, Zwetsloot M, Delory BM, Hennecke J, Andraczek K, Henning T, Mommer L, Weigelt A, Bergmann J. 2025. Revisiting the root economics space – its applications, extensions and nuances advance our understanding of fine-root functioning. *Plant and Soil*. doi: 10.1007/s11104-025-07379-6.

McGonigle TP, Miller MH, Evans DG, Fairchild GL, Swan JA. 1990. A new method which gives an objective measure of colonization of roots by vesicular-arbuscular mycorrhizal fungi. *New Phytologist* **115**: 495–501.

Meier IC, Tückmantel T, Heitkötter J, Müller K, Preusser S, Wrobe TJ, Kandeler E, Marschner B, Leuschner C. 2020. Root exudation of mature beech forests across a nutrient availability gradient: the role of root morphology and fungal activity. *New Phytologist* **226**: 583–594.

Meyer S, Angeli AD, Fernie AR, Martinoia E. 2010. Intra- and extra-cellular excretion of carboxylates. *Trends in Plant Science* **15**: 40–47.

Pasternak T, Kircher S, Palme K, Pérez-Pérez JM. 2023. Regulation of early seedling establishment and root development in *Arabidopsis thaliana* by light and carbohydrates. *Planta* **258**: 76.

Peterson RA. 2021. Finding optimal normalizing transformations via BESTNORMALIZE. *The R Journal* **13**: 310–329.

Phillips RP, Erlitz Y, Bier R, Bernhardt ES. 2008. New approach for capturing soluble root exudates in forest soils. *Functional Ecology* **22**: 990–999.

R Core Team. 2023. *R: a language and environment for statistical computing*. Vienna, Austria: R Foundation for Statistical Computing.

Ramakrishna P, Gámez-Arjona FM, Bellani E, Martin-Olmos C, Escrig S, De Bellis D, De Luca A, Pardo JM, Quintero FJ, Genoud C *et al.* 2025. Elemental cryo-imaging reveals SOS1-dependent vacuolar sodium accumulation. *Nature* **637**: 1228–1233.

Reich PB, Tjoelker MG, Pregitzer KS, Wright IJ, Oleksyn J, Machado JL. 2008. Scaling of respiration to nitrogen in leaves, stems and roots of higher land plants. *Ecology Letters* **11**: 793–801.

Roumet C, Birouste M, Picon-Cochard C, Ghestem M, Osman N, Vrignon-Brenas S, Cao KF, Stokes A. 2016. Root structure-function relationships in 74 species: evidence of a root economics spectrum related to carbon economy. *New Phytologist* **210**: 815–826.

Ryan PR, Delhaize E, Jones D. 2001. Function and mechanism of organic anion exudation from plant roots. *Annual Review of Plant Physiology and Plant Molecular Biology* **52**: 527–560.

Savage JA, Clearwater MJ, Haines DF, Klein T, Mencuccini M, Sevanto S, Turgeon R, Zhang C. 2016. Allocation, stress tolerance and carbon transport in plants: how does phloem physiology affect plant ecology? *Plant, Cell & Environment* **39**: 709–725.

Schneider CA, Rasband WS, Eliceiri KW. 2012. NIH IMAGE to IMAGEJ: 25 years of image analysis. *Nature Methods* **9**: 671–675.

Schneider HM, Strock CF, Hanlona MT, Vanhees DJ, Perkins AC, Ajmera IB, Sidhu JS, Mooney SJ, Browna KM, Lynch JP. 2021. Multiseriate cortical

sclerenchyma enhance root penetration in compacted soils. *Proceedings of the National Academy of Sciences, USA* **118**: e2012087118.

Schrader J, Nilsson J, Mellerowicz E, Berglund A, Nilsson P, Hertzberg M, Sandberg G. 2004. A high-resolution transcript profile across the wood-forming meristem of poplar identifies potential regulators of cambial stem cell identity. *Plant Cell* **16**: 2278–2292.

Sidhu JS, Ajmera I, Arya S, Lynch JP. 2023. *RootSlice* – a novel functional-structural model for root anatomical phenotypes. *Plant, Cell & Environment* **46**: 1671–1690.

Sidhu JS, Lopez-Valdivia I, Strock CF, Schneider HM, Lynch JP. 2024. Cortical parenchyma wall width regulates root metabolic cost and maize performance under suboptimal water availability. *Journal of Experimental Botany* **75**: 5750–5767.

Sidhu JS, Lynch JP. 2024. Cortical cell size regulates root metabolic cost. *The Plant Journal* **118**: 1343–1357.

Sun LJ, Ataka M, Han MG, Han YF, Gan DY, Guo YP, Xu TL, Zhu B. 2021. Root exudation as a major competitive fine-root functional trait of 18 coexisting species in a subtropical forest. *New Phytologist* **229**: 259–271.

Tjoelker MG, Craine JM, Wedin D, Reich PB, Tilman D. 2005. Linking leaf and root trait syndromes among 39 grassland and savannah species. *New Phytologist* **167**: 493–508.

Vives-Peris V, de Ollas C, Gómez-Cadenas A, Pérez-Clemente RM. 2020. Root exudates: from plant to rhizosphere and beyond. *Plant Cell Reports* **39**: 3–17.

de Vries FT, Williams A, Stringer F, Willcocks R, McEwing R, Langridge H, Straathof AL. 2019. Changes in root-exudate-induced respiration reveal a novel mechanism through which drought affects ecosystem carbon cycling. *New Phytologist* **224**: 132–145.

Wang M, Kong D, Mo X, Wang Y, Yang Q, Kardol P, Valverde-Barrantes OJ, Simpson MJ, Zeng H, Reich PB *et al.* 2024. Molecular-level carbon traits underlie the multidimensional fine root economics space. *Nature Plants* **10**: 901–909.

Wang X, Liu X, Chen S, Zhu J, Yuan Y, Zhu R, Chen K, Yang X, Wang X, Mo W *et al.* 2024. Elevational variation in anatomical traits of the first-order roots and their adaptation mechanisms. *Plant Diversity* **47**: 291–299.

Weigelt A, Mommer L, Andraczek K, Iversen CM, Bergmann J, Bruelheide H, Freschet GT, Guerrero-Ramírez NR, Kattge J, Kuyper TW *et al.* 2023. The importance of trait selection in ecology. *Nature* **618**: E29–E30.

Wen Z, White PJ, Shen J, Lambers H. 2022. Linking root exudation to belowground economic traits for resource acquisition. *New Phytologist* **233**: 1620–1635.

Weston LA, Ryan PR, Michelle W. 2012. Mechanisms for cellular transport and release of allelochemicals from plant roots into the rhizosphere. *Journal of Experimental Botany* **63**: 3445–3454.

Williams A, Langridge H, Straathof AL, Muhamadali H, Hollywood KA, Goodacre R, de Vries FT. 2021. Root functional traits explain root exudation rate and composition across a range of grassland species. *Journal of Ecology* **110**: 21–33.

Williams A, de Vries FT. 2020. Plant root exudation under drought: implications for ecosystem functioning. *New Phytologist* **225**: 1899–1905.

Wu S, Wang Y, Wang Z, Shrestha N, Liu J. 2022. Species divergence with gene flow and hybrid speciation on the Qinghai-Tibet Plateau. *New Phytologist* **234**: 392–404.

Xia M, Guo D, Pregitzer KS. 2010. Ephemeral root modules in *Fraxinus mandshurica*. *New Phytologist* **188**: 1065–1074.

Yang Q, Guo B, Lu M, Liu Y, Kardol P, Reich PB, Bardgett RD, Cornelissen JHC, Kraft NJB, Díaz S *et al.* 2025. Arbuscular mycorrhizal association regulates global root-seed coordination. *Nature Plants* **11**: 1759–1768.

Yuan Y, Li B, Gao X, Liu W, Li Y, Li R. 2022. Validation of cloud-gap-filled snow cover of MODIS daily cloud-free snow cover products on the Qinghai-Tibetan Plateau. *Remote Sensing* **14**: 5642.

Zadworny M, McCormack ML, Mucha J, Reich PB, Oleksyn J. 2016. Scots pine fine roots adjust along a 2000-km latitudinal climatic gradient. *New Phytologist* **212**: 389–399.

Zadworny M, McCormack ML, Żytkowiak R, Karolewski P, Mucha J, Oleksyn J. 2017. Patterns of structural and defense investments in fine roots of Scots pine (*Pinus sylvestris* L.) across a strong temperature and latitudinal gradient in Europe. *Global Change Biology* **23**: 1218–1231.

Zhang Y, Cao J, Lu M, Kardol P, Wang J, Fan G, Kong D. 2024. The origin of bi-dimensionality in plant root traits. *Trends in Ecology & Evolution* **39**: 78–88.

Zhang Y, Cao J, Yang Q, Wu X, Zhao Y, Kong D. 2023. The worldwide allometric relationship in anatomical structures for plant roots. *Plant Diversity* **456**: 621–629.

Zhao J, Guo B, Hou Y, Yang Q, Feng Z, Zhao Y, Yang X, Fan G, Kong D. 2024. Multi-dimensionality in plant root traits: progress and challenges. *Journal of Plant Ecology* **17**: rtae043.

Zhao Y, Xu F, Liu J, Guan F, Quan H, Meng F. 2019. The adaptation strategies of *Herpetospermum pedunculosum* (Ser.) Baill at altitude gradient of the Tibetan plateau by physiological and metabolomic methods. *BMC Genomics* **20**: 451.

Zheng Z, Wang C, Wang Y, Zhang Y, Valverde-Barrantes OJ, Zhang WH, Kong D. 2024a. Decoupling of uptake- and transport-related traits in absorptive roots across coexisting herbaceous species in alpine meadows. *Journal of Ecology* **112**: 770–783.

Zheng Z, Zhang Y, Li Z, Dong F, Chen L. 2024b. Two grasses differ in their absorptive root physiological traits and rooting depth under drought in an alpine steppe. *Annals of Botany* mcae151.

Zhou M, Bai W, Li Q, Guo Y, Zhang WH. 2021. Root anatomical traits determined leaf-level physiology and responses to precipitation change of herbaceous species in a temperate steppe. *New Phytologist* **229**: 1481–1491.

Zhou M, Bai W, Zhang Y, Zhang WH. 2018. A multi-dimensional variation pattern of root traits among coexisting herbaceous species in temperate steppes. *Journal of Ecology* **106**: 2320–2331.

Zhou M, Guo Y, Sheng J, Yuan Y, Zhang WH, Bai W. 2022. Using anatomical traits to understand root functions across root orders of herbaceous species in a temperate steppe. *New Phytologist* **234**: 422–434.

Supporting Information

Additional Supporting Information may be found online in the Supporting Information section at the end of the article.

Fig. S1 Monthly maximum temperature, monthly minimum temperature, and monthly mean rainfall.

Fig. S2 Phylogenetic relationship and distribution of absorptive root trait values.

Fig. S3 Overview of absorptive root sampling in the field.

Fig. S4 Linear regression between absorptive root diameter and cortex thickness, as well as absorptive root diameter and stele radius.

Fig. S5 Phylogenetically informed principal component analysis of absorptive root traits.

Fig. S6 Ordinary least squares regressions between specific root respiration and other root traits.

Fig. S7 Ordinary least squares regressions between absorptive root exudation rate and root morphological traits.

Fig. S8 Ordinary least squares regressions between acid phosphatase activity and root morphological traits.

Table S1 Absorptive root functions and their indicators.

Table S2 Dataset of herbaceous plants at the global level.

Table S3 Comparison of observed root tissue density and expected RTD of absorptive roots.

Table S4 Principal component analysis and phylogenetically informed principal component analysis.